The influence of anisotropic growth and geometry on the stress of solid tumors

Ariel Ramírez-Torres[a], Reinaldo Rodríguez-Ramos[b], José Merodio[c], Raimondo Penta[c], Julián Bravo-Castillero[b], Raúl Guinovart-Díaz[b], Federico J. Sabina[a], Catherine García-Reimbert[a], Igor Sevostianov[d], Aura Conci[e]

[a]*Instituto de Investigaciones en Matemáticas Aplicadas y en Sistemas (IIMAS). Universidad Nacional Autónoma de México, 01000 CDMX, Apartado Postal 20-126, México.*
[b]*Departamento de Matemáticas, Facultad de Matemática y Computación, Universidad de La Habana, 10400, La Habana, Cuba.*
[c]*Departamento de Mecánica de los Medios Continuos y T. Estructuras, E.T.S. de Caminos, Canales y Puertos, Universidad Politécnica de Madrid, 28040 Madrid, España.*
[d]*Department of Mechanical and Aerospace Engineering, New Mexico State University, P.O. Box 30001, Las Cruces, NM 88003, USA.*
[e]*Instituto de Computação. Universidade Federal Fluminense. CEP:24210-346, Río de Janeiro, Brasil.*

Abstract

Solid stresses can affect tumor patho-physiology in at least two ways: directly, by compressing cancer and stromal cells, and indirectly, by deforming blood and lymphatic vessels. In this work, we model the tumor mass as a growing hyperelastic material. We enforce a multiplicative decomposition of the deformation gradient to study the role of anisotropic tumor growth on the evolution and spatial distribution of stresses. Specifically, we exploit radial symmetry and analyze the response of circumferential and radial stresses to (a) degree of anisotropy, (b) geometry of the tumor mass (cylindrical versus spherical shape), and (c) different tumor types (in terms of mechanical properties). According to our results, both radial and circumferential stresses are compressive in the tumor inner regions, whereas circumferential stresses are tensile at the periphery. Furthermore, we show that the growth rate is inversely correlated with the stresses' magnitudes. These qualitative trends are consistent with experimental results. Our findings therefore elucidate the role of anisotropic growth on the tumor stress state. The potential of stress-alleviation strategies working together with anticancer therapies can result in better treatments.

Keywords: tumor modeling; anisotropic growth; stress; hyperelasticity.

1. Introduction

Tumor growth involves the generation of mechanical forces both within the tumor and between the tumor and the host tissue. The development of a tumor could be closely associated with the generation and accumulation of mechanical stresses [35, 37]. These mechanical forces, coupled with neovascularization, can induce abnormal solid and fluid stresses that facilitate tumor progression and hinder the response to various anti-cancer treatments ([17]). As shown in several experimental studies (see e.g. [11, 6, 7, 39]), mechanical stresses can determine in part the progression of solid tumors. Solid stresses ([17])) can affect tumor patho-physiology directly, by compressing cancer and stromal cells, and indirectly, by deforming blood and lymphatic vessels [37]. On one hand, cell compression can alters gene expression, cancer cell

Email addresses: ariel.ramirez@iimas.unam.mx (Ariel Ramírez-Torres), reinaldo@matcom.uh.cu (Reinaldo Rodríguez-Ramos), jose.merodio@upm.es (José Merodio), raimondo.penta@upm.es (Raimondo Penta), jbravo@matcom.uh.cu (Julián Bravo-Castillero), guino@matcom.uh.cu (Raúl Guinovart-Díaz), fjs@mym.iimas.unam.mx (Federico J. Sabina), cgr@mym.iimas.unam.mx (Catherine García-Reimbert), igor@nmsu.edu (Igor Sevostianov), aconci@ic.uff.br (Aura Conci)

proliferation, apoptosis and invasiveness, stromal cell function, and extracellular matrix synthesis and organization ([6, 39]). On the other hand, compression of blood and lymphatic vessels can reduce the delivery of oxygen, nutrients and drugs. Compromising the effectiveness of anti-cancer therapies ([22, 35]). Anti-cancer therapies by stress-relief have been proposed to improve and complement drug treatments delivery efficacy ([35, 16]). These strategies are based on the reduction of the stress levels, which causes reopening of compressed tumor blood vessels, thus leading to enhanced fluid and, in turn, drug transport within the tumor mass. In [36] it is shown that pharmacological depletion of tumor stroma with saridegib (i.e. an inhibitor of the sonic hedgehog pathway ([17])), alleviates stress levels and increases blood vessels diameter and tumor perfusion without affecting vascular density. In [21], the authors show that the use of saridegib improves the effectiveness of chemotherapy in murine pancreatic cancers and increases the mice survival rate. Furthermore, clinical studies in humans show that antiangiogenic agents can normalize tumor vasculature, so patients whose tumor blood perfusion increases survive longer ([16]). Morover, in [23] and [19], the authors solve the homogenized fluid and drug transport models developed in [34] and [24] for vascularized tumors, respectively. Their analysis, which was extended to mechanic deformations in [26], supports the argument that geometric regularization of the microvasculature improves transport of blood and advected drugs transported into the tumor mass. Cancer evolution is extremely complex and cannot be reduced only to its mechanical stress response; however some features in the tumor progression can be associated with the generation and accumulation of mechanical stresses.

An increased awareness of the mechanical response of a growing tumor mass can also contribute to a more informed design of anti-cancer therapies that rely on cancer tissue destruction, such as those based on ultasounds. For example, the High-Intensity Focused Ultrasound (HIFU) is a well-known technique which exploits ultrasounds to remove the malignat tissue. In fact, it has been successfully applied in the treatment of solid tumors (pancreas, liver, colon, etc.) ([1]). Although tissue destruction takes normally place via thermal ablation, the interest in mechanical HIFU (where ultrasounds are used to generate mechanical ablation) is increasing (see, e.g. [12]), and its working mechanisms are strongly related to the mechanical response of different tissue types. Moreover, mechanical forces can be used for medical simulations involving the discover of tumors ([18]). Our study is therefore motivated by the importance of stresses in determining tumors' progression and treatment. Given the lack of *in vivo* data, the development of theoretical investigations that can provide reliable predictions can support the design of effective anti-cancer treatments.

In the present work we model the tumor mass as a growing hyperelastic material and investigate the role of anisotropic tumor growth on tumor stresses. Growth take place when conversion of mass is present from one constituent to another, and once a mixture is considered then there are subtle issues concerning boundary conditions that have to be clearly discussed (see e.g. [13, 14, 15]). In particular, we assume that the solid tumor is surrounded by a compressible, isotropic and hyperelastic medium. We extend the analysis reported in [32] by performing for the first time a parametric analysis in terms of (a) degree of anisotropy, (b) tumor shape (cylindrical versus spherical), and (c) tumor types that are characterized by different mechanical properties. In fact, cylindrical and spherical tumor shapes have been experimentally observed as shown in [9] and [41], respectively.

The reminder of this work is organized as follows. In Section 2 we describe the multiplicative decomposition of the deformation gradient tensor to account for both the elastic response and growth of the tumor contributions. The theory of materials with evolving natural configurations developed by Rajagopal and co-workers (see for instance [28]) is used since it permits to model growth and stress-induced deformation separately. In Section 3 we introduce the Ciarlet's strain energy function which is exploited to model the hyperelastic response of the tumor. In Section 4 we introduce the balance equations for mass and linear momentum. In section 5 we describe the adopted evolution law for growth. In Section 6 we summarize the mathematical model and then specialize it for spherical and cylindrical geometries, assuming radial symmetry in both cases. In Section 7 we present and discuss our results obtained via numerical simulations of the mathematical model. In Section 8 we present our conclusions.

2. Multiplicative decomposition of the deformation gradient tensor

Tumor growth is modeled using the multiplicative decomposition of the deformation gradient tensor $\mathbf{F}$. In fact, the essential difficulty in formalizing the dynamics of biological growth is the simultaneous modeling of the change in mass and how the latter affects the stresses. The theory of materials with evolving natural configurations ([13])overcomes this complexity by separating such stress contributions ([3]). Then,

$$\boldsymbol{F} = \boldsymbol{F}_{el}\boldsymbol{G}, \tag{1}$$

where $\mathbf{F}_{el}$ describes the local deformation from the natural configuration κ_{el} (the natural configuration is the reference configuration chosen to represent the elastic responses of the material) to the actual configuration κ_t and it is associated with the elastic response of the material. On the other hand, the tensor $\boldsymbol{G}$ is directly connected to growth, and therefore it is referred to as the growth tensor. Now, since $\boldsymbol{G}$ is introduced, an additional constitutive equation must be postulated. In this sense, it is known that most soft biological tissues possess a highly anisotropic microstructure. Thus, we take the following form for the growth tensor ([32, 20])

$$\boldsymbol{G} = g_2\boldsymbol{I} + (g_1 - g_2)\boldsymbol{n}_g \otimes \boldsymbol{n}_g, \tag{2}$$

where $\mathbf{I}$ is the identity tensor and g_1 and g_2 account for parallel and perpendicular anisotropic contributions with respect to $\boldsymbol{n}_g$, respectively.

3. Constitutive relations

According to experimental evidences, tumors can be considered as compressible materials ([11]). In particular, the response from the natural configurations is modeled considering the tumor as an isotropic, compressible and non-linear hyperelastic solid, where the material response is the same for each natural configuration. As a matter of fact, several constitutive functions have been used in the modeling of tumor tissue. In the recent study by [40], the authors showed that the experimental stress-strain response of two tumor types (MCF10CA1a and SW620) is better fitted to an exponential constitutive equation compared to the widely used neo-Hookean and Blatz-Ko models. However, they found that the evolution of stress and growth rate of the tumor are independent from these specific constitutive relations. This is the reason why we adopt the simplified Ciarlet strain energy function ([5]).

$$\psi = \frac{\lambda}{4}\left(\mathit{III}_{\boldsymbol{B}} - \ln \mathit{III}_{\boldsymbol{B}} - 1\right) + \frac{\mu}{2}\left(I_{\boldsymbol{B}} - \ln \mathit{III}_{\boldsymbol{B}} - 3\right), \tag{3}$$

where λ and μ are the Lamé's constants and $I_{\mathbf{B}}$ and $\mathit{III}_{\mathbf{B}}$ are the first and third principal invariants of the left Cauchy-Green deformation tensor $\mathbf{B} = \boldsymbol{F}\boldsymbol{F}^T$, respectively. Now, like κ_{el} is chosen as the reference configuration representing the elastic responses of the material and assuming that material properties do not change during growth. The Cauchy stress tensor can be written as ([5]),

$$\boldsymbol{\sigma}_{el} = \boldsymbol{\sigma}(\boldsymbol{B}_{el}) = \frac{2\rho_r}{\sqrt{\mathit{III}_{\boldsymbol{B}_{el}}}}\frac{\partial \psi_{el}}{\partial \boldsymbol{B}_{el}}\boldsymbol{B}_{el}, \tag{4}$$

where ρ_r denotes the density field in the Lagrangian description and $\boldsymbol{B}_{el} = \boldsymbol{F}_{el}(\boldsymbol{F}_{el})^T$.

4. Balance equations

In the present work, the well-known mass balance equation with a source term is used ([29]),

$$\dot{\rho} + \nabla \cdot (\rho \boldsymbol{v}) = \rho\Gamma, \tag{5}$$

where ρ is the mass density, $\boldsymbol{v}$ is the velocity field and $\rho\Gamma$ is the mass supply rate. In particular, ([30])

$$\rho = \frac{\rho_r}{J_{el}}, \tag{6}$$

where $J_{el} = \det \boldsymbol{F}_{el}$. Moreover, Γ has the following form,

$$\Gamma = \mathrm{tr}(\dot{\boldsymbol{G}}\boldsymbol{G}^{-1}). \tag{7}$$

On the other hand, ignoring inertial terms, the linear momentum equation read as ([29])

$$\nabla \cdot \boldsymbol{\sigma}_{el} = \boldsymbol{0}, \tag{8}$$

where body forces and interaction terms have been neglected. Recently, the action of body forces and interaction terms on tumor growth has been investigated in [31] and [32], respectively. Focusing on the adhesion mechanisms between cells and the extracellular matrix, the authors in [27] have proposed constitutive models for the interaction terms.

5. Evolution law for growth

Tumor mechanical responses and interactions with the surrounding tissue influence its growth. In this sense, the process of growth can not be unlinked to stresses and deformations of the body. Then, an evolution law that accounts for these contributions needs to be postulated. In particular, any proposed law must obey the constraint (6). On the other hand, considering the dissipation principle of [2] and following the procedure made in [30],

$$\Gamma = \mathrm{tr}\left[\boldsymbol{K}^{-1}\left(-\psi\boldsymbol{I} + J_{el}(\boldsymbol{F}_{el})^T\boldsymbol{\sigma}(\boldsymbol{F}_{el})^{-T} + \boldsymbol{M}\right)\right], \tag{9}$$

where $\boldsymbol{K}$ is a symmetric positive definite tensor and $\boldsymbol{M}$ governs the growth process and is referred to as the accretive forces tensor ([31] and [2]). Thus, (6) together with (2) and $\boldsymbol{n}_g = \boldsymbol{e}_r$, gives

$$\frac{\dot{g}_1}{g_1} + 2\frac{\dot{g}_2}{g_2} = \Gamma. \tag{10}$$

In particular, in the present work it is assumed that $g_1 = \alpha g_2$, with α being a positive constant. Notice that α is a model parameter that accounts for the degree of anisotropy. In particular, the isotropic formulation of the model is obtained for $\alpha = 1$. Then, Eq. (10) rewrites,

$$\dot{g}_2 = \frac{\Gamma}{3} g_2. \tag{11}$$

Now, it is reasonable to assume that growth is proportional to the nutrient concentration n. In this sense, if a body grows, a stimulus must be provided as well as a supply of energy, in this case driven by the nutrients. We denote by n_e the part of the nutrient concentration that provides the energy for tumor growth. Then, as the energy for growth supplied externally is related to the accretive forces and is referred to the tensor $\boldsymbol{M}$, we postulate that $\boldsymbol{M} = \gamma n_e \boldsymbol{I}$, where γ is a model parameter ([32]). On the other hand, it is introduced an expression to relate tumor growth with the levels of solid stresses. Following [32], we take

$\boldsymbol{K} = (\beta(n - n_d)(1 + \varepsilon\bar{\sigma}))^{-1}\,\boldsymbol{I}$, where β is a positive constant, $n > n_d$ with n_d being the part of n dedicated to carry out functions, like plastics (forming the structure of the organism as well as allowing its growth) and regulators (controlling the chemical reactions resulting from the cell metabolism). Besides, ε is a constant that describes the dependence of Γ on the stress and $\bar{\sigma} = \mathrm{tr}(\boldsymbol{\sigma})/3$ is the bulk solid stress ([40]). We remark that other expressions for Γ are also possible. For instance, to model contact inhibition in [10] is considered that the growth term depends on a switch mechanism based on the compression levels, using a monotonic mollifier of the step function.

6. Mathematical model

The mathematical model can be summarized using equations (8) and (11), together with a diffusion equation describing the evolution of the nutrients concentration at a material point. Specifically,

$$\nabla \cdot \boldsymbol{\sigma}_{el} = 0, \tag{12}$$

$$\dot{g}_2 = \frac{\Gamma}{3} g_2, \tag{13}$$

$$\dot{n} = \delta \Delta n - 3(\zeta + n)\frac{\dot{g}_2}{g_2}, \tag{14}$$

with δ being a diffusion constant and ζ a proportionality constant ([32]). The system (12)-(14) is solved with the following initial and boundary conditions

$$\begin{array}{ll} \underline{\text{Initial conditions}}\ (t = 0) & \underline{\text{Boundary conditions}}\ (t > 0) \\ \boldsymbol{u} = \boldsymbol{u}_0, & [[\boldsymbol{n} \cdot \boldsymbol{u}]] = 0, \quad \text{on } \partial_{\boldsymbol{u}} \\ n = n(\boldsymbol{u}, t), & [[\boldsymbol{n}\boldsymbol{\sigma}_{el}]] = \boldsymbol{0}, \quad \text{on } \partial_{\boldsymbol{\sigma}} \\ \boldsymbol{G} = \boldsymbol{I}, & n = c, \qquad \text{on } \partial, \end{array} \tag{15}$$

where $\boldsymbol{u}$ is the displacement vector field, $\boldsymbol{u}_0$ is the initial displacement, $\boldsymbol{n}$ is the outward normal vector to the tumor surface, $[[\bullet]]$ represents the jump evaluated across the interface, $\partial = \partial_{\boldsymbol{u}} \cup \partial_{\boldsymbol{\sigma}}$ is the tumor boundary and c is a positive constant. We specify directly the boundary conditions for n in the tumor center later on, when we specialize the model assuming radial symmetry.

6.1. Cylindrical kinematics

We investigate tumor growth and solid stresses for a tumor with cylindrical geometry. Some tumors adopt this particular shape, for example, ductal carcinoma in situ (DCIS) of the breast represents the initial growth stage of breast cancer ([8]). At this point, the tumor is non invasive, being confined by the basement membrane of the duct. In particular, we describe and formulate the mathematical model using a cylindrical coordinate system. Then, (R, Θ, Z) and (r, θ, z) give the cylindrical coordinates in the reference and deformed configurations respectively, where $R,\ r > 0$, $-\pi/2 \leq \Theta,\ \theta < \pi/2$ and $Z,\ z > 0$. Moreover, it is assumed that the deformation of the body will be given only in the radial direction, i.e., $r = r(R, t)$, $\Theta = \theta$ and $Z = z$.

6.2. Spherical kinematics

In [11], it is shown that tumors growing in free suspension adopt a spherical shape, while those growing within an agarose gel take an ellipsoidal geometry due to anisotropic stresses exerted by the gel. In particular, the incorporation of an isotropic elastic law in the model suggest the fact that the tumor is modeled in a spherical shape. In particular, we describe and formulate the mathematical model using a spherical coordinate system. Then, (R, Θ, Φ) and (r, θ, ϕ) give the spherical coordinates in the reference and deformed configurations respectively, where $R,\ r > 0$, $-\pi/2 \leq \Theta,\ \theta < \pi/2$ and $-\pi \leq \Phi, \phi < \pi$. Moreover, it is assumed that the deformation of the body will be given only in the radial direction, i.e., $r = r(R, t)$, $\Theta = \theta$ and $\Phi = \phi$.

6.3. Dimensionless formulation of the mathematical model

The process of non-dimensionalization is considered to rescale the system of variables according to their characteristic quantities. Particularly, tumor radius is rescaled by a characteristic length $L := 10^{-1}cm$ and the time scale by $\tau := L^2D^{-1}$, where $D := 1.157407 \times 10^{-7}cm^2s^{-1}$ ([4]). The density is rescaled by $\rho_r = 10^{-2}Kgcm^{-3}$, the nutrient concentration by its corresponding value at the boundary (c) and the stress by μ. The non-dimensional parameters of the model are summarized as follows:

$$\begin{aligned} &R = L\tilde{R}, \quad r = L\tilde{r}, \quad \rho = \rho_r\tilde{\rho}, \quad n = c\tilde{n}, \quad n_e = c\tilde{n}_e, \quad n_d = c\tilde{n}_d, \quad \zeta = c\tilde{\zeta}, \quad \sigma = \mu\tilde{\sigma}, \\ &\Gamma = \tau^{-1}\tilde{\Gamma}, \quad \gamma = \mu c^{-1}\tilde{\gamma}, \quad \beta = (\mu c)^{-1}\tilde{\beta}, \quad \varepsilon = \mu^{-1}\tilde{\varepsilon} \quad \text{and} \quad \delta = D\tilde{\delta}. \end{aligned} \tag{16}$$

According to Eqs. (12)-(14) the system to be solved has the form,

$$\frac{(\tilde{\sigma}^{rr}_{el})'}{\tilde{r}'} + m\frac{\tilde{\sigma}^{rr}_{el} - \tilde{\sigma}^{\theta\theta}_{el}}{\tilde{r}} = 0, \tag{17}$$

$$\dot{g}_2 = \frac{\tilde{\beta}(\tilde{n} - \tilde{n}_d)(1 + \tilde{\varepsilon}\tilde{\bar{\sigma}})}{3}\mathrm{tr}\left(\left(-\tilde{\psi}\boldsymbol{I} + J^{el}(\boldsymbol{F}^{el})^T\tilde{\boldsymbol{\sigma}}(\boldsymbol{F}^{el})^{-T} + \tilde{\gamma}\tilde{n}_e\boldsymbol{I}\right)g_2\right), \tag{18}$$

$$\dot{\tilde{n}} = \tilde{\delta}\left(\frac{1}{\tilde{r}'}\left(\frac{\tilde{n}'}{\tilde{r}'}\right)' + m\frac{\tilde{n}'}{\tilde{r}\tilde{r}'}\right) - 3(\tilde{\zeta} + \tilde{n})\frac{\dot{g}_2}{g_2}, \tag{19}$$

where $\bullet' = \partial \bullet /\partial\tilde{R}$, $\tilde{\sigma}^{rr}_{el} = \alpha\rho_r\tilde{R}g_2^3\left(\left((\tilde{r}')^2/(\alpha^2g_2^2) - 1\right) + (\lambda/(2\mu))\left((\tilde{r}')^2\tilde{r}^2/(\alpha^2\tilde{R}^2g_2^6) - 1\right)\right)/(\tilde{r}'\tilde{r})$ and $\tilde{\sigma}^{\theta\theta}_{el} = \alpha\rho_r\tilde{R}g_2^3\left(\left(\tilde{r}^2/(\tilde{R}^2g_2^2) - 1\right) + (\lambda/(2\mu))\left((\tilde{r}')^2\tilde{r}^2/(\alpha^2\tilde{R}^2g_2^6) - 1\right)\right)/(\tilde{r}'\tilde{r})$.

In Eqs. (17) and (19) the constant m ($m = 1, 2$), indicates the corresponding mathematical model, i.e. if $m = 1$ the mathematical model for the cylindrical deformation described in Section 6.1 is obtained, otherwise if $m = 2$, we are in presence of the spherical deformation problem defined in Section 6.2 . In particular, the system (17)-(19) is solved with the following initial and boundary conditions,

$$\begin{array}{ll} \underline{\text{Initial conditions}}\ (t = 0) & \underline{\text{Boundary conditions}}\ (t > 0) \\ \tilde{r} = \tilde{r}_0, & [[\tilde{r}]] = 0, \quad \text{on } \partial_{\boldsymbol{u}} \\ \tilde{n} = \frac{1}{2c}\left(\left(\frac{L\tilde{R}}{3}\right)^2 + 1\right), & [[\tilde{\sigma}^{rr}]] = 0, \quad \text{on } \partial_{\sigma} \\ \boldsymbol{G} = \boldsymbol{I}, & \tilde{n}' = 0, \quad \text{in } \boldsymbol{o}, \\ & \tilde{n} = 1, \quad \text{on } \partial, \end{array} \tag{20}$$

where "$\boldsymbol{o}$" denotes the tumor center.

7. Numerical simulations

In this section, the numerical results corresponding to the dimensionless mathematical model (17)-(20) are discussed. In particular, the numerical method was implemented in Python. As a strategy to obtain numerical solutions of the proposed models the time is assumed discrete, which allows to have a discrete version of the time-continuous problems.

The objective of this work is not to study the effect of stresses on tumor growth. We refer the reader to [32] where mechanical modulation of growth by solid stresses are investigated. In the present study, growth and stresses are studied for various tumor types and tumor shapes (cylindrical and spherical) under the effect of the stress applied by a surrounding medium. The tumor-surrounding host tissue is considered as a hyperelastic and compressible solid material which is deformed by the growing solid tumor. In particular, the deformation of the external tissue take place only in the radial direction and the Ciarlet strain energy function given by (3) is selected to represent its stress-strain response. For the external medium, the bulk modulus provided in [33] for 0.5% agarose gel, i.e. $\kappa_h = 0.01199898\ Ncm^{-2}$ and $\nu_h = 0.18$, are chosen. The present model is not constrained to the particular form of the stress law for the surrounding solid, that it just addresses the interactions between the tumor and the surrounding host tissue.

7.1. Cylindrical geometry

Mechanical material properties measured for the murine mammary adenocarcinoma MCaIV in [36] are used, i.e. the shear modulus $\mu = 0.4999575\ N/cm^2$ and the bulk modulus $\kappa = 0.66661\ N/cm^2$. The Poisson ratio is set to $\nu = 0.2$ ([30] and [40]). We also fix the dimensionless parameters to $\tilde{\beta} = 1/\hat{\mu}$, with $\hat{\mu}$ representing the numerical value of μ (i.e. without the dimension); $\tilde{n}_d = (1 - 2 \times 10^{-5})\tilde{n}$, $\tilde{\gamma}\tilde{n}_e = 10^{-1}\tilde{n}$, $\tilde{\varepsilon} = 1.875159$, $\tilde{\delta} = 10^{-9}$ and $\tilde{\zeta} = 10^{-1}$.

In Fig. 1 (A) the evolution of the breast tumor type MCaIV's radius versus time is displayed for the case of the isotropic formulation, i.e. for $\alpha = 1$. At first glance, it is noticed that even when the model does not consider a lack of nutrients during the tumor evolution, its growth slows down in time. This behavior is due to the presence of the host tissue at the tumor boundary which is modulating its growth. In addition, in Fig. 1 (B) and (C), the distribution of the stresses for different instants of time are shown. In this particular case of isotropic growth, we can note that tumor stresses are almost constants in space. Now, we consider an

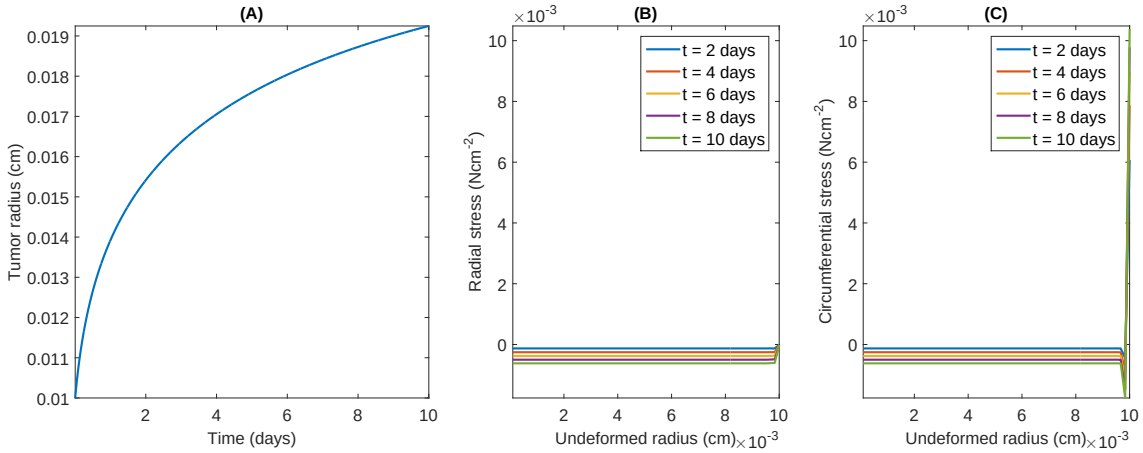

Figure 1: (A) Radius evolution of the murine mammary adenocarcinoma MCaIV versus time with $\alpha = 1$.(B) Radial stress and (C) circumferential stress for different instants of time for the murine mammary adenocarcinoma MCaIV.

anisotropic formulation, i.e. we set $\alpha \neq 1$. As observed in Fig. 2, the anisotropic form of the growth tensor $\boldsymbol{G}$ influences the tumor stress behavior. In a previous work ([32]), it is shown how this specific anisotropic

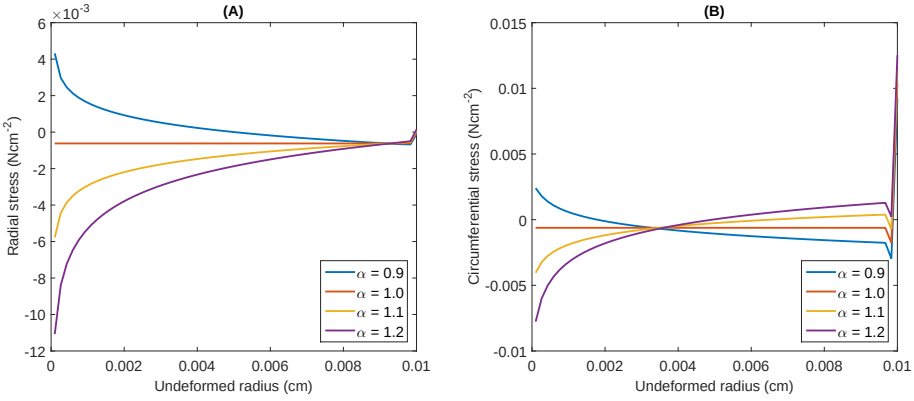

Figure 2: Effect of the anisotropy on (A) radial stress and (B) circumferential stress of the breast tumor type MCaIV for the fixed instant $t = 10$ days.

form of the tensor $\boldsymbol{G}$ (Eq. (2)) influences the growth of a tumor. Here, in a same way the anisotropic

property affects tumor stresses. As pointed out in [17], stress can be direction dependent, that is they can be compressive in the interior of the tumor in both the radial and circumferential directions, whereas at the interface with the host tissue, radial stresses can be compressive, and circumferential stresses can be tensile. As shown in Fig. 2, this behavior is predicted by the mathematical model when anisotropy is considered, particularly for $\alpha > 1$ (i.e. when $g_1 > g_2$). Specifically, for $\alpha > 1$, radial and circumferential stresses are compressive in the spatial interior, whereas at the interface with the host tissue, circumferential stresses are tensile. We remark that the value of the stresses at the periphery are constrained to the election of the surrounding medium strain energy and mechanical constants.

7.2. Spherical geometry

The present study can be extended in order to compare growth and stresses for the same type of tumor but with different shapes. The murine mammary adenocarcinoma MCaIV is chosen as an example. In this sense, in Fig. 3 (A) it is shown the radius evolution in time for the tumor type MCaIV with cylindrical (blue) and spherical (red) shapes. Interestingly, with cylindrical geometry it reaches a higher radius. Moreover, it is noticed that radial stresses for both geometries are almost identical (see Fig. 3 (B) and (C) and (D) first line). However, in Fig. 3 (B) and (C) and (D) (second line), it is observed that circumferential stresses differ,

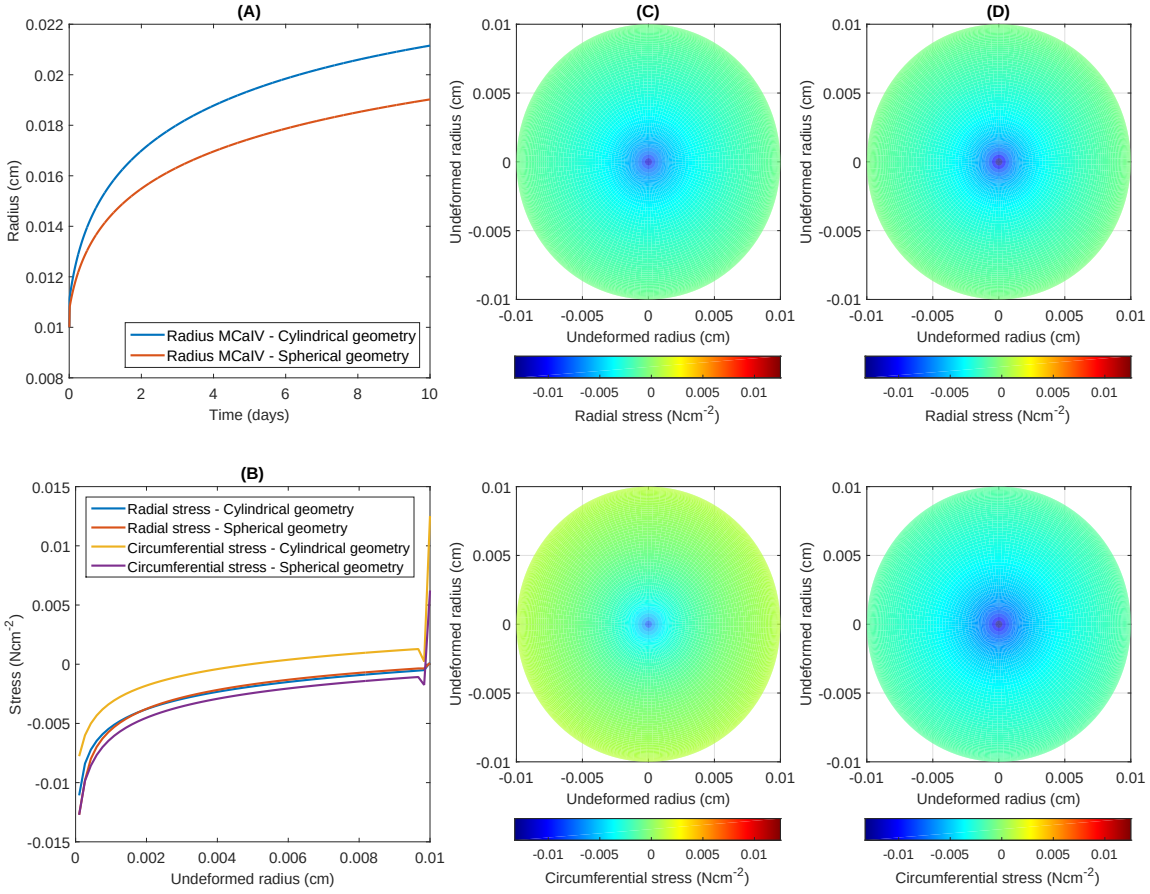

Figure 3: (A) Comparison between the radius evolution of the murine mammary adenocarcinoma MCaIV for different geometries and $\alpha = 1.2$. (B) Radial and circumferential stress distributions for the fixed instant $t = 10$ days of the murine mammary adenocarcinoma MCaIV for different geometries. (C) Horizontal strip of color corresponds to the radial (first line) and circumferential (second line) stress values for the tumor type MCaIV with cylindrical shape. (D) Horizontal strip of color corresponds to the radial (first line) and circumferential (second line) stress values for the tumor type MCaIV with spherical shape.

not in behavior but in numerical values. Specifically, circumferential stresses are more compressive when considering a spherical shape for the tumor.

7.3. Comparison of results

In order to continue with the study the spherical shape for the tumor is chosen. The present model predicts experimental findings obtained by [36], where tumors with higher stress levels exhibit a slower growth, presumably owing to reduced cancer cell proliferation and increased apoptosis. In particular, the mechanical materials properties given in Tab. 1 for three tumor types ([36]) are considered. In the experimental study

Table 1: Mechanical material properties of the tumor types considered.

Tumor Type (Cancer cell line)	**Bulk modulus** κ (Ncm^{-2})	**Shear modulus** μ (Ncm^{-2})
Melanoma (MU89)	0.2533118	0.189984
Colon (LS174T)	0.399966	0.2999745
Glioma (U87)	2.66644	1.99983

by [36], tumors with higher stress levels exhibited a slower growth. In this sense, in Fig. 4 is observed a comparison between the growth of the tumors considered in Tab. 1. It is evident, that in the same lapse

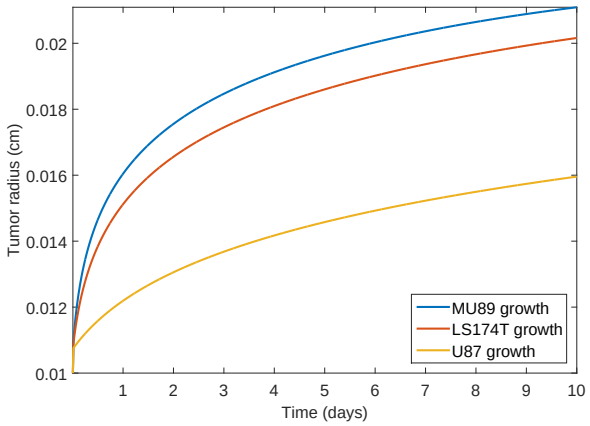

Figure 4: Comparison between the radius evolution of the tumor types considered in Tab. 1 with $\alpha = 1.2$.

of time, the human melanoma MU89 grows more than the human colon adenocarcinoma LS174T and the human gliobastoma U87. In fact, the numerical results agree with the study reported in [36]. Specifically, the tumor with the higher stress levels (human gliobastoma U87) is the one that grows slower, meanwhile the tumor type with the lower stress levels (human melanoma MU89) grows faster. This can be observed in Fig. 5, where it is shown the radial and circumferential stresses for the human melanoma MU89 and the human gliobastoma U87.

8. Conclusions

In the present work, a continuum mechanical model is proposed to study the role of anisotropic tumor growth on tumor stresses. We found that radial and circumferential stresses are compressive in the spatial interior, whereas at the periphery, circumferential stresses are tensile. These numerical results are consistent with experimental findings. Moreover, the results agree with the fact that tumors with higher stress levels grow slower, meanwhile tumors with lower stress levels grow faster. Given the fact that the current treatment

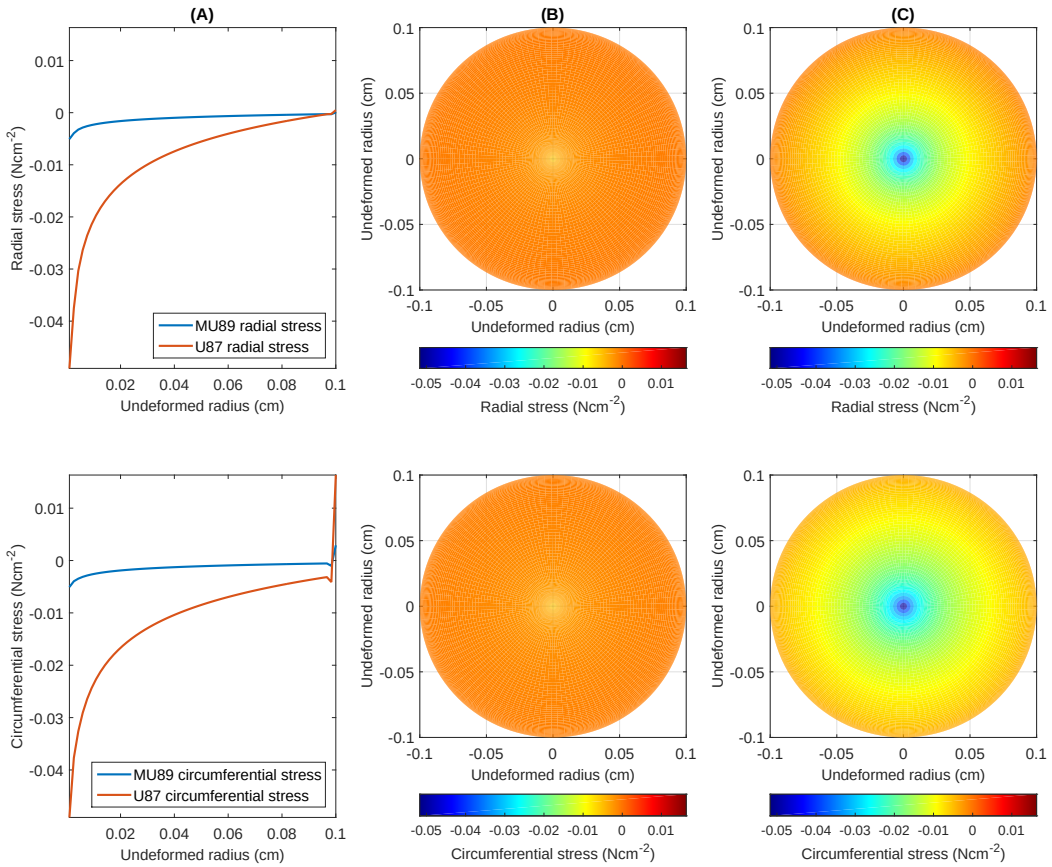

Figure 5: (A) Radial and circumferential stress distributions for the fixed instant $t = 10$ days and $\alpha = 1.2$. (B) Horizontal strip of color corresponds to the radial (first line) and circumferential (second line) stress values for the human melanoma MU89. (C) Horizontal strip of color corresponds to the radial (first line) and circumferential (second line) stress values for the human gliobastoma U87.

situation still needs to innovate, mechanical models could generate big potential to find new paths for cancer treatment.

Challenging further developments include (a) the extension of the model to vascularized tumors, (b) the generalization to a poroelastic mechanical behavior of the malignant mass (see, e.g. [25] for a homogenized model of (linear) growing poroelastic materials), (c) the coupling with suitable mathematical models which describe transport of macromolecules (see, e.g. the homogenized models [34, 24] for vascularized, rigid and non-growing tumors), as well as nanoparticles delivery (see [38] for a review on the subject), and (d) the impact of tumor stresses on geometry and hydraulic properties of the blood vessels.

A systematic theoretical study of mathematical models which account for tumor stresses can contribute to the development of new approaches for cancer diagnosis and treatment and the reduction of invasive clinical trials.

Acknowledgments

AR gratefully acknowledges the Program of Postdoctoral Scholarships of DGAPA from UNAM, Mexico. JM and RP acknowledge support from the Ministry of Economy in Spain under the project reference DPI2014-58885-R. Thanks to the Project (7515) Métodos Físico-Matemáticos para el estudio de nuevos materiales y la propagación de ondas. Aplicaciones. Also, we thanks to Departamento de Matemáticas y

Mecánica IIMAS-UNAM for their support and Ramiro Chávez Tovar and Ana Pérez Arteaga for computational assistance. A.C. is grateful to CNPq (Projects INCT-MACC and 303240/2015-6).

References

[1] Ahrar, K., Matin, S., Wood, C. G., Wallace, M. J., Gupta, S., Madoff, D. C., Rao, S., Tannir, N. M., Jonasch, E., Pisters, L. L., Rozner, M. A., Kennamer, D. L. and Hicks, M. E., 2005. "Percutaneous Radiofrequency Ablation of Renal Tumors: Technique, Complications, and Outcomes". *Journal of Vascular and Interventional Radiology*, Vol. 16, pp. 679–688.

[2] Ambrosi, D. and Guana, F., 2007. "Stress-modulated growth". *Mathematics and Mechanics of Solids*, Vol. 12, pp. 319–343.

[3] Ambrosi, D. and Mollica, F., 2002. "On the mechanics of a growing tumor". *International Journal of Engineering Science*, Vol. 40, pp. 1297–1316.

[4] Ambrosi, D. and Mollica, F., 2004. "The role of stress in the growth of a multicell spheroid". *Journal of Mathematical Biology*, Vol. 48, pp. 477–499.

[5] Bertram, A., 2008. *Elasticity and plasticity of large deformations. An introduction*. 2nd Ed., Springer, Heidelberg.

[6] Cheng, G., Tse, J., Jain, R. K. and Munn, L. L., 2009.. "Micro-environmental mechanical stress controls tumor spheroid size and morphology by suppressing proliferation and inducing apoptosis in cancer cells". *PLoS ONE*, Vol. 4, pp. e4632.

[7] Demou, Z. N., 2010. "Gene Expression Profiles in 3D Tumor Analogs Indicate Compressive Strain Differentially Enhances Metastatic Potential". *Annals of Biomedical Engineering*, Vol. 38, pp. 3509–3520.

[8] Franks, S.J., Byrne, H. M., King, J. R., Underwood, J. C. E. and Lewis, C. E., 2003.. "Modelling the early growth of ductal carcinoma in situ of the breast". *Journal of Mathematical Biology*, Vol. 47, pp. 424–452.

[9] Franks, S.J., Byrne, H. M., Mudhar, H. S., Underwood, J. C. E. and Lewis, C. E., 2003. "Mathematical modelling of comedo ductal carcinoma in situ of the breast". *Mathematical Medicine and Biology*, Vol. 20, pp. 277–308.

[10] Galle, J., Preziosi, L. and Tosin, A., 2009.. "Contact inhibition of growth described using amultiphase model and an individual cell based model". Vol. 22, pp. 1483–1490.

[11] Helmlinger, G., Netti, P. A., Lichtenbeld, H. C., Melder, R. J. and Jain, R. K., 1997. "Solid stress inhibits the growth of multicellular tumour spheroids". *Nature Biotechnology*, Vol. 15, pp. 778–783.

[12] Hoogenboom, M., Eikelenboom, D., den Brok, M.H., Heerschap, A., Fütterer, J.J., Adema, G.J., 2015. Mechanical high-intensity focused ultrasound destruction of soft tissue: working mechanisms and physiologic effects. Ultrasound in medicine & biology 41, 1500–1517.

[13] Humphrey, J. D., Rajagopal, K. R., 2002. "A constrained mixture model for growth and remodeling of soft tissues". *Mathematical Models and Methods in Applied Sciences*, Vol. 12, pp. 407–430.

[14] Humphrey, J. D., Rao, I.J., Rajagopal, K. R., 2002. "A mixture model for growth and remodeling in soft tissues". *ASME-PUBLICATIONS-BED*, Vol. 50, pp. 645–646.

[15] Rao, I.J., Humphrey, J. D., Rajagopal, K. R., 2003. "Biological Growth and Remodeling: A Uniaxial Example with Possible Application to Tendons and Ligaments". *Computer Modeling in Engineering and Sciences*, Vol. 4, pp. 439–456.

[16] Jain, R. K., 2013. "Normalizing tumor microenvironment to treat cancer: bench to bedside to biomarkers". *Journal of Clinical Oncology*, Vol. 31, pp. 2205–2218.

[17] Jain, R. K., Martin, J. D. and Stylianopoulos, T., 2014. "The role of mechanical forces in tumor growth and therapy". *Annual Review of Biomedical Engineering*, Vol. 16, pp. 321–346.

[18] Jeon, S., Choi, S. and Harders, M., 2012. "Rendering Virtual Tumors in Real Tissue Mock-Ups Using Haptic Augmented Reality". *IEEE Transactions on Haptics*, Vol. 5, pp. 77–84.

[19] Mascheroni, P., Penta, R., 2017. "The role of the microvascular network structure on diffusion and consumption of anticancer drugs". *International Journal for Numerical Methods in Biomedical Engineering*, e2857.

[20] Menzel, A. and Kuhl, E., 2012. "Frontiers in growth and remodeling". *Mechanics Research Communications*, Vol. 42, pp. 1–14.

[21] Olive, K. P., Jacobetz, M. A., Davidson, C. J., Gopinathan, A. and McIntyr, D., 2009. "Inhibition of Hedgehog signaling enhances delivery of chemotherapy in a mouse model of pancreatic cancer". *Science*, Vol. 324, pp. 1457–1461.

[22] Padera, T. P., Stoll, B. R., Tooredman, J. B., Capen, D., di Tomaso, E. and Jain, R. K., 2004. "Pathology: Cancer cells compress intratumour vessels". *Nature*, Vol. 427, pp. 695.

[23] Penta, R., Ambrosi, D., 2015. The role of the microvascular tortuosity in tumor transport phenomena. Journal of theoretical biology 364, 80–97.

[24] Penta, R., Ambrosi, D., Quarteroni, A., 2015. Multiscale homogenization for fluid and drug transport in vascularized malignant tissues. Mathematical Models and Methods in Applied Sciences 25, 79–108.

[25] Penta, R., Ambrosi, D., Shipley, R.J., 2014. Effective governing equations for poroelastic growing media. The Quarterly Journal of Mechanics and Applied Mathematics 67, 69–91.

[26] Penta, R., Merodio, J., 2017. Homogenized modeling for vascularized poroelastic materials. Meccanica, 1–23.

[27] L. Preziosi and Tosin, A., 2009. "Multiphase and multiscale trends in cancer modelling". *Mathematical Modelling of Natural Phenomena*, Vol. 4, pp. 1–11.

[28] Rajagopal, K. R., 1995. "Multiple configurations in continuum mechanics". *Reports of the institute for computational and applied mechanics 6*, University of Pittsburgh.

[29] Rajagopal, K. R. and Tao, L., 1995. *Mechanics of Mixture*. Singapore; River Edge, NJ: World Scientific.

[30] Ramírez-Torres, A., Rodríguez-Ramos, R., Glüge, R., Bravo-Castillero, J., Guinovart-Díaz, R. and Rodríguez-Sanchez, R., 2013. "Biomechanic approach of a growing tumor". *Mechanics Research Communications*, Vol. 51, pp. 32–38.

[31] Ramírez-Torres, A., Rodríguez-Ramos, R., Merodio, J., Bravo-Castillero, J., Guinovart-Díaz, R. and Alfonso, J. C. L., 2015. "Action of body forces in tumor growth". *International Journal of Engineering Science*, Vol. 89, pp. 18–34.

[32] Ramírez-Torres, A., Rodríguez-Ramos, R., Merodio, J., Bravo-Castillero, J., Guinovart-Díaz, R. and Alfonso, J. C. L., 2015. "Mathematical modeling of anisotropic avascular tumor growth". *Mechanics Research Communications*, Vol. 69, pp. 8–14.

[33] Roose, T., Netti, P. A., Munn, L. L., Boucher, Y. and Jain, R. K., 2003. "Solid stress generated byspheroid growth estimated using a linear poroelasticity model". *Microvascular Research*, Vol. 66, pp. 204–212.

[34] Shipley, R.J., Chapman, J., 2010. Multiscale modelling of fluid and drug transport in vascular tumors. Bulletin of Mathematical Biology. 72, 1464–1491.

[35] Stylianopoulos, T. and Jain, R. K., 2013. "Combining two strategies to improve perfusion and drug delivery in solid tumors". *Proceedings of the National Academy of Sciences USA*, Vol. 110, pp. 18632–18637.

[36] Stylianopoulos, T., Martin, J. D., Chauhan, V. P., Jain, S. R. and Diop-Frimpong, B., 2012. "Causes, consequences, and remedies for growth-induced solid stress in murine and human tumors". *Proceedings of the National Academy of Sciences USA*, Vol. 109, pp. 15101–15108.

[37] Stylianopoulos, T., 2017. "The solid mechanics of cancer and strategies for improved therapy". *Journal of Biomechanical Engineering*, Vol. 139, 021004-1.

[38] Taffetani, M., de Falco, C., Penta, R., Ambrosi, D., Ciarletta, P., 2014. Biomechanical modelling in nanomedicine: multiscale approaches and future challenges. Archive of Applied Mechanics 84, 1627–1645.

[39] Tse, J. M., Cheng, G., Tyrrell, J. A., Wilcox-Adelman S. A. and Boucher, Y., 2012. "Mechanical compression drives cancer cells toward invasive phenotype". *Proceedings of the National Academy of Sciences USA*, Vol. 109, pp. 911–916.

[40] Voutouri, C., Mpekris, F., Papageorgis, P., Odysseos, A. D. and Stylianopoulos, T., 2014. "Role of constitutive behavior and tumor-host mechanical interactions in the state of stress and growth of solid tumors". *PLoS ONE*, Vol. 9, pp. e104717.

[41] Weiswald, L.B., Bellet, D. and Dangles-Marie,V., 2015. "Spherical Cancer Models in Tumor Biology". *Neoplasia*, Vol. 17, pp. 1-15.